INTERNATIONAL JOURNAL OF ADVANCE RESEARCH, IDEAS AND INNOVATIONS IN TECHNOLOGY

ISSN: 2454-132X
Impact factor: 4.295
(Volume3, Issue3)
Available online at www.ijariit.com

Tumor and Edema Segmentation Using Efficient MFCM and MRG Algorithm

Rehna Kalam
Kerala University
rehanakalam988@gmail.com

M. Abdul Rahman
Kerala University
rehman_paika@Yahoo.com

Abstract**: Momentarily, categorizing of brain tumor and segmentation is truly an exciting task in MRI. Numerous researchers work in generating divergent plus interesting techniques and algorithms for this specified work of medical image processing. On behalf of enhancing a precise brain tumor extraction, we provide an effective methodology for both classification and segmentation i.e., separation of brain MRI images as well as labeling of brain MRI images in terms of edema, tumor, white matter (WM), gray matter (GM) plus cerebrospinal fluid (CSF). At this instant and in our recommended system of brain tumor detection encompasses six segments, i.e. pre-processing, filtering, Image registration, Feature extraction, Classification, Segmentation. At this moment, in the case of preprocessing, the input MRI image is firstly fetched from the MRI database and as well subjected to skull stripping for rejecting the undesirable area from the image. In addition, by the utilizing Gaussian filter, the skull stripped image has been smoothened. Subsequently, by utilizing Automatic image registration, the filtered images are recorded into one coordinate system wherever the movement of the head is a situation often encountered during the imaging process. Shape, intensity, and texture are the features that will be extricated from the registered images.On the basis of extricated features, the Brain MRI images are characterized by normal or abnormal images. Finally, by utilizing the modified FCM segmentation algorithm tumor portion is extracted and edema is segmented applying modified region enhancing the abnormal images. Therefore in case of a normal image, the Gray matter, the white matter, and the cerebrospinal fluid can be segmented. The outcomes are analyzed for illustrating the representation of the suggested classification plus segmentation methodology with prevailing techniques.

Keywords: Skull Stripping, Filtering, Image Registration, Feature Extraction, Classification, Segmentation.

I. INTRODUCTION

The brain is a complicated structure which is a lenient, gentle non-replaceable, however, flexible mass of tissue. Neoplasm is nothing but the tumor or a solid lesion created by an unusual development [1] of cells that resembles of a swelling. This is a bunch of tissue which develops out of control of the common forces that normalizes development. Tumors may ruin rest powerful cells of the brain. It is incidentally injury vigorous cells through crowding another portion of the brain and also reason inflammation, brain swelling and also create pressure inside the skull [2]. Obviously, the brain tumors that are known to be Primary brain tumors are the one which can develop from cells in the brain or beside from the cover of the brain. A metastatic brain tumor is known to be secondary brain tumor whereas it happens by spreading of cancer cells to brain from the primary cancer cells in one or other portion of the body [3]. Brain tumors encompass of tumors in the pivotal spinal canal or else within the cranium. Spontaneous defects detection in MRI is beneficial in numerous diagnostic and also therapeutic applications calculated tomography and alsoMRI are the two imaging modalities [4] that researchers with medical practitioners for analyzing the brain through observing at it noninvasively [5]. Several times, the tumor segmentation and also classification turn tougher due to blurred boundaries and MR images quantity. As the brain is protected by the skull, thence, a premature finding of brain tumor is only thinkable while tools of diagnostic are focused intracranial cavity at [6].

Magnetic resonance imaging (MRI) has turned a broadly-utilized technique of superior-quality medical imaging; particularly in brain imaging in which MRI's soft tissues contrast [7] plus noninvasive ness hold benefits [8]. A salient utilization of MRI data is following the brain tumor size since it answers (or else does not) for treatment. Hence, a mechanized and dependable technique for extracting tumor might be a beneficial tool [9]. Skull stripping associates the non-brain tissues' removal [10]. However, this is one among the significant methods of neuron imaging analysis. Most of the skull stripping handles the brain like a single associated region isolated from non-brain tissues through a rim of cerebrospinal fluid (CSF) [11]. Actually even with great resolution, T1

Weighted MR images, squeaky connections betwixt the brain and also other cranial structure prevail in the Dura form and connective tissue lining venous sinuses [12]. Image-related tumor detection utilizes one or else more algorithms like the key modeling. Hardly few may discover edges; a number may find shapes though others may discover other components. Though developments in camera sensing, computational technologies and developments in tumor detection utilizing are playing a vital role in the intelligent medical community [13] and such features are tremendously active in the research field of such aforementioned community.

In contemporary years, medical imaging plus soft computing have generated pivotal advancements in the brain tumor segmentation's field [14]. Typically, several unusual brain tumor tissues can be unearthed uncomplicatedly with brain tumor segmentation techniques [15]. But precise and also reproducible segmentation consequences and also a demonstration of abnormalities are not rectified all the way. As brain tumor segmentation has great influence on diagnosis, checking, treatment formation or trials of patients, and clinical [16]. In the former research of medical tumor finding, the algorithms have directly utilized the conventional techniques of image processing (Like edge finding plus region developing) according to gray intensities of images [17]. Recently, the human brain segmentation in MRI images is probably through supervised methods of k-nearest neighbor, Artificial neural networks, support vector machine(SVM) and the overall unsubstantiated classification [18] methodologies of self-organization map(SOM) and fuzzy C-means algorithm [19] have been employed for labeling the normal or otherwise pathological T2 subjective MRI images [20].

The rough draft erection of the paper is systematized as follows: Section 2 analyses the associated works regarding the proposed technique. In sections 3, a brief explanation of the recommended methodology is provided, section 4 evaluates the Experimental outcome and section 5 proffers conclusion to the paper.

II. RELATED WORK

Obviously, a brain tumor has been a bulk of tissue which was arranged through a gradual gathering of anomalous cells and it is substantial for classifying brain tumors by (MRI) i.e.; Magnetic Resonance Imaging for treatment. A Perfect classification of brain MRI was presented by Anitha *et.al* [1]. Information recognized by anatomical structures and also potential typical tissues were given by brain tumor segmentation on MRI which was significant to handle, such recommended system utilized the adaptive pillar K-means algorithm for efficacious apportionment and the classification technique is executed by the two-tier classification method. In the case of a suggested system, primarily the self-organizing map neural network trains the structures derived from the wavelet of discrete transform blend wavelets and more the resultant filter traits are consequently qualified by the K-nearest neighbor and as well the testing method was also accomplished in two stages. The intended two-tier classification system categorized the brain tumors in double training method which provides desirable performance through conventional classification technique.

An automated dependable system was demonstrated by Quaratul*et.al* [2] for the detection of brain tumors. Recommended system was oriented for tumor region abstraction and brain tumor detection since it was a multi-stage structure. In the beginning, noise elimination was implemented as the preprocessing scheme on brain MR images. Moreover, the texture aspects were a derivative of such noise free brain MR images. Then the suggested system's phase was classification according to these derived features. Ensemble related SVM classification was utilized. Supplementary in excess of 99% accurateness was accomplished through the classification part. The suggested system derives tumor region from the tumorous images utilizing multi-step segmentation, after classification. The initial phase was skull removal plus brain region extraction. Next phase was isolating tumor region from the usual brain cells utilizing FCM clustering. Consequences of the suggested technique provide that tumor region was derived somewhat precisely.

The MRI images' classification of general and pathological brain settings posed a demand from technological plus medical perception, as MR imaging targeted on soft tissue anatomy plus created a huge information set and these could perform as a mirror reflecting the settings of the brain. An innovative methodology by combining wavelet entropy related spider web designs, in addition, a probabilistic neural network was suggested by Saritha*et.al* [3] aimed at the labeling of MRI brain images respectively. Next to this juncture, the two-step system for grouping employs (1) Probabilistic neural network for categorization and (2) wavelet entropy related spider web plots for attaining the feature. Moreover, the spider web plot was a geometric structure derived by employing the wavelet approximation factors 'entropy and hence the computed regions are exploited as a feature set for labeling.

A spontaneous algorithm for brain stroke plus tumor lesion recognition and also segmentation utilizing single-spectral MRI was presented by Nooshin*et.al* [4]. At such case, an algorithm recognized to be histogram-related gravitational optimization algorithm (HGOA) which utilizes a novel intensity-related segmentation process, by means of such method an improved gravitational optimization algorithm on histogram evaluation consequences can be achievable. The mathematical demonstrations and the convergence benchmarks of the enhanced optimization algorithm were explicitly presented. Applying this algorithm, brain image was split into a variant number of regions that would be branded as a lesion or else healthy.

Ahmad chadad*et.al* [5] has suggested a novel technique of skull stripping for the axial slices obtained from MRI. Afterward, by utilizing multi-level threshold segmentation according to histogram evaluation, the brain tumor can be identified. Eventually, the skull-stripping technique was employed by means of adaptive morphological operations procedure. As such, techniques predicted an empirical threshold over the calculation of arena of brain tissue. It was engaged on the registering of non-contrast T1-weighted (T1-WI) with its associating fluid attenuated inversion recovery sequel. Next, we utilized multi-thresholding segmentation (MTS) technique which is suggested by Otsu.

III. PROPOSED METHODOLOGY

The goal of our suggested system in this exploration proffers prompt categorization of usual plus unusual images and segmentation in usual plus unusual of MRI. In order to carry out preprocessing, the input Brain MR images are derived from the database. Filtration of Preprocessed images is done utilizing Gaussian filtering and recorded by employing automatic image registration. Subsequently, Brain MR Images in which the components of shape, intensity plus texture are extricated from the recorded images and regarding the derived attributes such brain images are characterized by normal as well abnormal images. At that time, from the normal images

we can get white matter, gray matter and also Cerebrospinal fluid and from the abnormal images we can get tumor plus edema region and it is extracted using well-organized algorithms. The suggested task block diagram is mentioned in fig. 1,

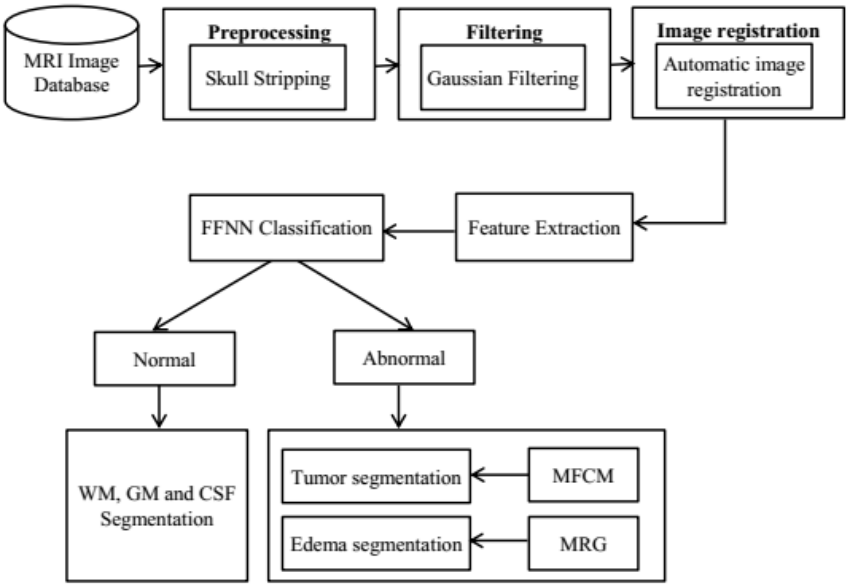

Fig. 1 Proposed block diagram

3.1 Pre-Processing

3.1.1 Skull stripping

Skull stripping is the process in which from the MR brain images, eradication of non-brain tissues can be carried out. In our recommended work, an efficient process which is used for the purpose of the pre-processing is the Skull stripping methodology. Generally, the skull-stripping means a procedure involved for removing the skull from the MR images in the brain region. It partitions the brain from the scalp, skull, vein, meninges and other nearby brain parts. The following steps are organized to discard the skull from the Brain images.

Step.1: Get the input image (I) from the database db .

Step.2: Add variance to the input image (I) by applying the following equation.

$$NI = \sin(I^{3}/100)^{2} + \frac{1}{20} \times rand(size\,of\ I) \tag{1}$$

Step.3: Perform the orthotic function on the input image (I) and the outcoming image is represented as $O(I)$.

Step.4: Locate the optimum valued pixel (m) from the input image (I) and analyze the limit (max (mx_c) & min (mn_c)) of the color range existing on the image $O(I)$.

Step.5: Evaluate the generalized image with the assistance of Equation. (2)

$$n_r I = (OI - mx_c)/(mx_c - mn_c) \tag{2}$$

Step.6: Evaluate the level of the normalized image (τ) by applying the Otsu's methodology for the orthotic image $O(I)$.

step.7: Compute the threshold for forecasting the filtered image ($f(I)$) engaging the below equation.

$$\tau = n_r I \times (mx_c - mn_c) + mn_c \tag{3}$$

Step.8: Add the pixels into the filtered image $f(I)$ whose values exceed the threshold analyzed in step 6.

Step.9: Estimate the threshold (τ_1) by using the Otsu's methodology for the image analyzed from the input image (I) by using equation (4).

$$\tau = Otsu's\left(I/m\right) \times m \tag{4}$$

Step.10: Add the pixels into the filtered image ($f_1(I)$) whose values exceed the threshold evaluated in step.9.

Step.11: Substitute the pixels of the filtered image ($f(I)$) attained in step.6 by the filtered image achieved in $f_1(I)$.

Step.12: Perform the opening operation of the morphological function and locate the area for diverse regions in the resulting image achieved in step.12, bounding box (pixels in the edges).

Step.13: Choose the region at which the area exceeds 50000 pixels and its resultant bounding box.

Step.14: Perform the closing operation of morphological function on the image attained in step.13 employing the MATLAB function.

Step.15: Generate a mask with the size of $W \times W_i$ and fill the picked region within its related bounding box employing the generated mask.

Step.16: Locate the position of the one valued pixels and substitute the one valued pixels by the original pixels in that position of the input image I .The resulting image $Sk_t(I)$ represents the skull stripped image and it is employed for further processing.

3.1.2 Gaussian Filtering

In the case of Gaussian Filtering, the Gaussian noise can be eliminated by using a filter known as a Gaussian filter. At this point, The Gaussian Smoothing operator ensures a weighted average of environments pixels in accordance with a Gaussian distribution. The weights proffer greater importance for pixels adjacent the edge (diminishes edge blurring). The quantity of smoothing is restrained by σ (huger σ for more concentrated smoothing). Sigma denotes the quantity of blurring. Moreover, the radius slider is utilized for controlling how huge the template is. Huge values for sigma will only proffer huge blurring for bigger template sizes. Noise is added utilizing the sliders. Both blurring of images and also erasing noise plus detail can be done by means of Gaussian filtering. The representation of such Gaussian function is mentioned below as follow:

$$g(a,b) = \frac{1}{2\pi\sigma^2} \bullet e^{-(\frac{a^2+b^2}{2\sigma^2})} \tag{5}$$

Where σ denotes the standard deviation in case of Gaussian distribution. The Gaussian distribution has been presumed to hold a mean of 0. Gaussian smoothing is very efficient for eliminating Gaussian noise.

3.1.3 Image registration

All patients' images will be noted down to the same coordinate system. T1 weighted MR image is selected like the reference image and furthermore, we have recorded the other channels on it amidst subjects employing an Automatic image registration [26].

3.2 Features Extraction

In general, there exist several features such as Shape features, Intensity features and Texture features while Shape features comprising of Area, perimeter, and circularity likewise Intensity features comprises of Mean, variance and standard deviation similarly Texture features comprising of Contrast, energy, correlation, and homogeneity are utilized to designate the content of the image. The following are the features, employed for the efficient categorization of multi objects.

3.2.1 Shape feature

Area:

An area's image is resolved through the quantity of pixels prevailing amidst the image. Shape components of the area and also perimeter will be computed from the images. The area of a segmented image can be calculated utilizing the equation provided below,

$$Area = A = \frac{i(h)}{i(w)} \tag{6}$$

Where $i(h)$ is an image height, $i(w)$ is image width.

Perimeter:

The perimeter of a apportioned image is calculated utilizing the provided equation below,

$$perimeter = P = 2(i(h) + i(w)) \tag{7}$$

Circularity:

Circularity of the region in term of shape is denoted by applying the following equation.

$$C_r = 4\pi \frac{A}{P^2} \tag{8}$$

Where, C_r is the circularity, A is area and P is perimeter.

3.2.2 Intensity feature

Mean:

The mean or average intensity values of pixels are denoted by this feature.

$$\mu_j = \frac{1}{N}\sum_{i=1}^{N} y_{ji} \tag{9}$$

Standard deviation and variance:

It signifies contrast of every level of the image. It is measured by utilizing mean values of image plus pixel values of every level.

$$\sigma_j = \sqrt{\frac{1}{N}\sum_{i=1}^{N}(y_{ji} - \mu_j)^2} \tag{10}$$

Variance is defined as the square of standard deviation and it is represented by

$$Variance = V = \sigma_j^2 \tag{11}$$

3.2.3 Texture feature

Contrast ($\hat{C}$):

It proceeds with the measure of the intensity contrast betwixt a pixel and its neighbor through the complete image. In addition, contrast is 0 for a continuous image.

$$C = \sum_{y,z} |y-z|^2 \, P(y,z) \tag{12}$$

Where, C represents the contrast and $P(y,z)$ is the pixel at location (y,z)

Homogeneity (H):

Yields a value which computes the relationship of the distribution of features in the GLCM to the GLCM diagonal.

$$H = \sum_{y,z} \frac{P(y,z)}{1+|y-z|} \tag{13}$$

Energy:

Energy (E) is signified as the degree of extent of pixel pair iterations. It computesthe homogeneity of an image. While pixels are very equivalent, the energy value is huge. It is signified in equation (21) like,

$$E = \sqrt{\sum_{y=0}^{N-1} \sum_{z=0}^{N-1} P(y,z)^2} \tag{14}$$

Consider the co-occurrence matrix can be characterized by y and z coefficients of, $P(y,z)$ that is the element of co-occurrence matrix at the aforementioned coordinates y and z, whereas *N* signifies the dimensions of such co-occurrence matrix.

Correlation

Correlation has been statistical measures of how fine matching of predicted values is done with the actual values. This feature calculates exactly how a pixel is correlated to its neighborhood. It is defined as the measure of gray tone linear dependencies in the image. Correlation is denoted as follow,

$$C_n = \frac{\sum_{y=o}^{N-1} \sum_{z=0}^{N-1} (y,z) \, P(y,z) - \mu_a \mu_b}{\sigma_a \sigma_b} \tag{15}$$

Where, μ_a and μ_b are the means σ_a and σ_b are the standard deviations correspondingly.

3.3 Classification

3.3.1 FFBNN classifier

The derived feature set is delivered to the classifier known to be Feed Forward Back Propagation Neural Network (FFBNN) classifier for the activity of training. In the phase of training, the derived components are provided for the FFBNN network. The FFBNN network is trained well by such derived features. The 8 features of area (A), perimeter (P), circularity (C_r), mean (μ_j), variance (V), standard deviation (σ_j), contrast ($\hat{C}$), energy (E), correlation (C_n), homogeneity (H_m)are derived from the processed image and are furnished as inputs to the Feed Forward Back Propagation Neural Network classifier for training and classification purpose. The FFBNN is formulated with eight input units rendering to the derived features, concealed units, and one output unit. Figure 2 shows the structure of FFBNN classifier.

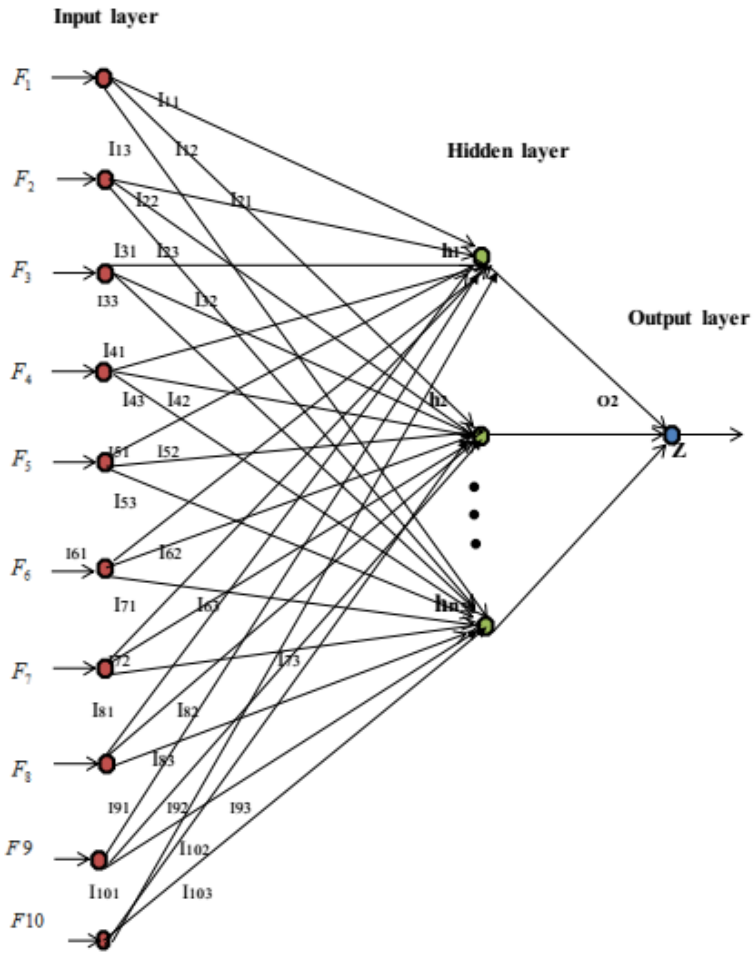

Fig. 2 Structure ofFFBNN

1. *The bias function of the neural network.*

Assign input weights to each neuron excluding the neurons present in the input layer. The scheduled bias function plus activation function for the neural networks are demonstrated as follows; in these, Bias function is considered as the product of weights plus inputs.

$$b(f) = \alpha + \sum_{n=1}^{h} (i(\hat{C}) + i(\mu_j) + i(A) + i(C_n) + i(E) + i(H_m) + i(P) + i(C_r) + i(\sigma_j) + i(V) + i(\mu_j)) \tag{16}$$

In bias function $A, \hat{C}, C_n, \sigma_j, \mu_j, E, H_m, V, P$, and C_r are the derived features.

2. Activation functions for the neural network:

Activation function can be represented by a non-linear function

$$H = \frac{1}{1 + \exp^{-b(f)}} \tag{17}$$

3. Calculation of learning error of the neural network obtained is given below:

$$Z = \frac{1}{s} \sum_{n=0}^{s-1} r_n - t_n \tag{18}$$

In which, Z is the FFBNN network output, r_n *and* t_n are the required and actual outputs and s represents the complete number of neurons of the concealed layer. The occurred mistake during the FFNN training method is diminished by the back propagation algorithm. Here, the neural network (n_r) effect is demonstrated in the following Equation (19).

$$result = \begin{cases} Abnormal, n_r \geq \breve{\upsilon}, \\ normal, n_r < \breve{\upsilon} \end{cases} \tag{19}$$

When the neural network output overtakes the threshold value $(\breve{\upsilon})$ then the particular input image is handled as normal. Or else, it is recognized as an unusual image.

3.4 Segmentation

Segmentation is a technique of splitting an image into divergent sections comprising every pixel with identical components. Formerly the categorization of brain images takes place in terms of normal and abnormal images. Moreover, the tumor region and edema region is separated from the categorized abnormal images while the white matter (WM), Gray matter (GM) and also Cerebrospinal fluid (CSF) is separated from the categorized normal images.

3.4.1 Tumor Segmentation from abnormal images using MFCM

The tumor is assigned from the abnormal images utilizing the algorithm namely Modified Fuzzy C-Means (MFCM) algorithm. The MFCM algorithm is typically utilized to cluster while the performance in the MFCM relies upon the choice of first cluster center or else membership value. The MFCM algorithm commences with a series of actual cluster centers. The MFCM algorithm allows pixels for every category by utilizing fuzzy memberships.

$$J_{\sigma n} = \sum_{i=1}^{I}\sum_{j=1}^{J}(v_{ij})^{n}\frac{\left\|p_i - q_j\right\|^2}{\sigma_i} \tag{20}$$

In Eqn. (20), p_i denotes the derived image, q_j is the j cluster center and n has been the constant value.

Where σ_i is the weighted mean distance in cluster I, and is provided by,

$$\sigma_i = \left\{\frac{\sum_{j=1}^{k} v_{ij}^{n}\left\|p_i - q_j\right\|^2}{\sum_{j=1}^{k} v_{ij}^{n}}\right\}^{1/2} \tag{21}$$

The membership function symbolizes the probability that the pixel relates to a particular cluster. On account of, the FCM algorithm the possibility is rendering to the distance between the pixel and every single individual cluster center of the feature domain. The membership functions and the cluster centers are represented by the equations (22) and (23).

$$v_{ij} = \frac{1}{\sum_{l=1}^{J}\left(\frac{\left\|p_i - q_j / \sigma_i\right\|}{\left\|p_i - q_l / \sigma_i\right\|}\right)^{\frac{2}{n-1}}} \tag{22}$$

The clusters centroid values is computed by using the equation (23)

$$z_j = \frac{\sum_{i=1}^{I} v_{ij}^{n} . x_i}{\sum_{i=1}^{I} v_{ij}^{n}} \tag{23}$$

Iterate the algorithm till the coefficients' modification betwixt two iterations is no more than ξ, for the provided sensitivity threshold.

$$\max_{ij}\left\|V_{ij}^{(k)} - V_{ij}^{(k+1)}\right\| < \psi \tag{24}$$

In equation (14), ψ is a termination benchmarking betwixt 0 and 1, in which δ are the repetition steps? Iterate the steps till effective clustering attained. Thus by the MFCM, the tumor image is apportioned.

3.4.2 Edema segmentation from abnormal images using MRG

Normally, the Region developing technique designates a tarnished technique for the image segmentation that includes choice of the seed point. In the segmentation process, the adjacent pixels are compared with the original seed points for analyzing according

to particular situations, if the adjacent pixels are appended to the region or not. The seed point choice constitutes a salient work in the apportionment. Nonetheless, the typical Region Growing process selects the seed points by arranging the intensity threshold that suffers from deficiencies of the noise or else deviation in intensity that effect in the over-segmentation or else holes. Additionally, the shadings of actual images may not be distinguished by such methods. Having a view for overwhelming the associated demands, theModified region growing (MRG) technique is adopted through considering the intensity and also orientation thresholds by the pre-processed images for execution of such features in the assortment of seed points. The methodology of the amended region developing method is exemplified in procedures as described below:

Step 1: Calculate the gradient in the image for both x axis $(\hat{g}_{ip})$ plus $(\hat{g}_{iq})$ y axis.

Step 2: Create the gradient vector GV through combining the gradient values as demonstrated in the below Equation:

$$GV = \frac{1}{1 + \left(\hat{g}_{ip}^{\,2} + \hat{g}_{iq}^{\,2}\right)} \tag{25}$$

Step 3: Modify the gradient vector values which are normally in radians into degrees to achieve the values of orientation.

Step 4: Segment the image into grids sg_i .

Step 5: Lay down the intensity threshold $\left(I_{(th)}\right)$ and orientation threshold $\left(O_{(th)}\right)$.

Step 6: In respect of every grid sg_i , carry on the following procedures in step 7 till the number of grids attains the total number of grids for an image.

Step 7(a): Locate the histogram h_g of every pixel in sg_i .

Step 7(b): Decide the most frequent histogram of the $sg_i^{\,th}$ grid and represent it as $Freq_{(h_g)}$.

Step 7(c): Choose any pixel, as per $Freq_{(h_g)}$ and allocate that pixel as the seed point having the intensity $\left(I_p\right)$ and Orientation $\left(O_p\right)$.

Step 7(d): Let us consider the adjacent pixels possessing the intensity $\left(I_n\right)$ and also its orientation $\left(O_n\right)$.

Step 7(e): Locate the intensity and orientation variance of those pixels p and n .

$$\text{(i.e) } diff_{\text{int}} = \left\| I_p - I_n \right\| \tag{26}$$

$$\text{And} \qquad diff_{orient} = \left\| O_p - O_n \right\| \tag{27}$$

Step 7(f): If $diff_{\text{int}} \le I_{(th)}$ && $diff_{orient} \le O_{th}$, then add the related pixel to the region and the region is grown, otherwise, move to step 7(h).

Step 7(g): Examine whether all the pixels are added to the region. If true, move to step 6, else move to step 7(h).

Step 7(h): Re-evaluate the region and locate the new seed points and perform the procedure from step 7(a).

Step 8: End the entire procedure.

Employing the Modified Region Growing procedure, the Edema region is segmented from the attained tumor images. Thus the accurate tumor region is achieved independently.

3.4.3 Segmentation of WM, GM, and CSF from normal images

The segmentation of White matter (WM), Gray matter (GM), and Cerebrospinal fluid (CSF) regions from the normal images can be done by means of the following steps,

Preprocessing: Following are the preprocessing steps that can be applied in the normal image for the purpose of segmentations.

1) Apply Gaussian noise in the normal image.
2) If the image size is less than 3 means, then convert the image into gray to index and gray to RGB.

White matter and gray matter segmentation steps

1) Filtering such as Gaussian filtering is applied to the preprocessed image
2) Applying 2D convolution in the filtered image
3) Applying gradient in the image
4) Applying gray thresholding
5) Applying morphological operation
6) At the end, removing the small object from binary image and outcomes with the gray matter plus white matter segments individually.

CSF segmentation phases:

1) Converts the preprocessed image into double format
2) Then apply noise using following formula,

$$y = \sin(img^{\,3}/100)^2 + 0.05 * randn(size(img)) \tag{28}$$

The segmented CSF region is attained by the following equation,

$$CSF = orthofit(y) \tag{29}$$

By employing the above steps, and hence the white matter, gray matter and CSF are segmented from the achieved normal images.

IV. RESULT AND DISCUSSION

The suggested brain MRI categorization and also segmentation was executed in the working platform of MATLAB (version 14) with machine configuration that follows:

Processor: Intel core i7
CPU Speed: 3.20 GHz
OS: Windows 7
RAM: 4GB

In this section, the experimental results attained for the suggested method are provided. The publically conceivable MRI image data set was utilized for the assessment. Fig.3 to 8 presents the sample images derived from the database, pre-processing the image utilizing skull stripping and also filtering the image utilizing Gaussian filter. Image registration is engaged in the filtered images and also classified as normal or abnormal images by applying to FFNN classifier. GM, WM, and CSF are dispensed from the categorized usual images and as well the tumor region and edema region is dispensed from the unusual images.

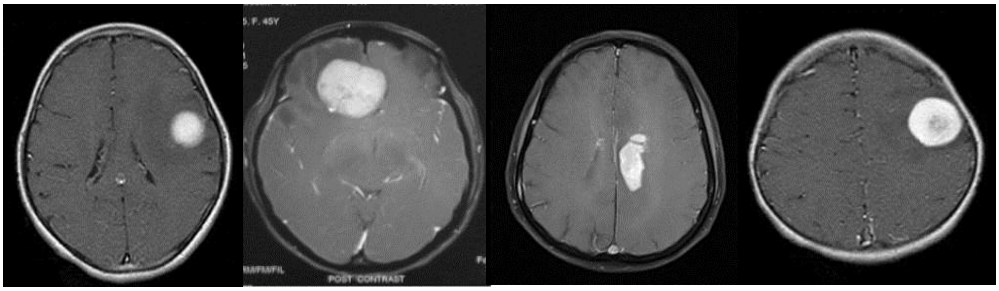

Fig.3 illustrates the sample images taken from the database

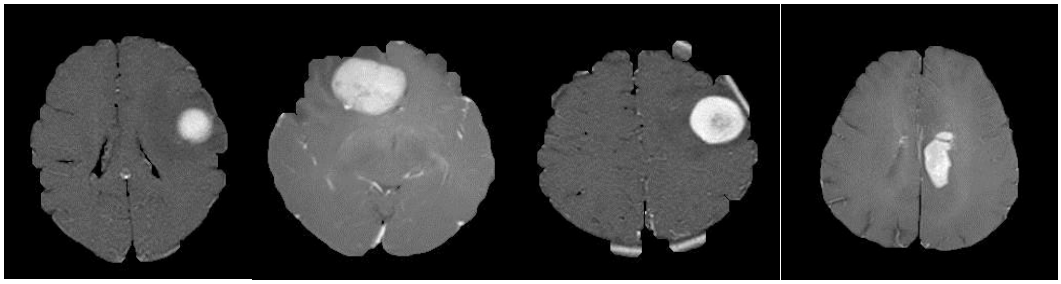

Fig. 4 skull stripped images

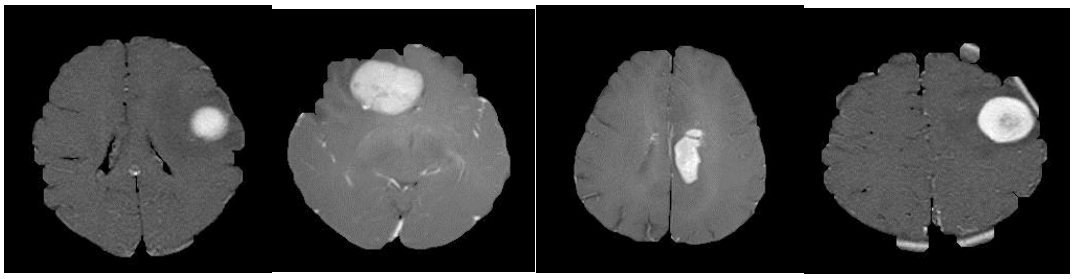

Fig. 5 filtered images

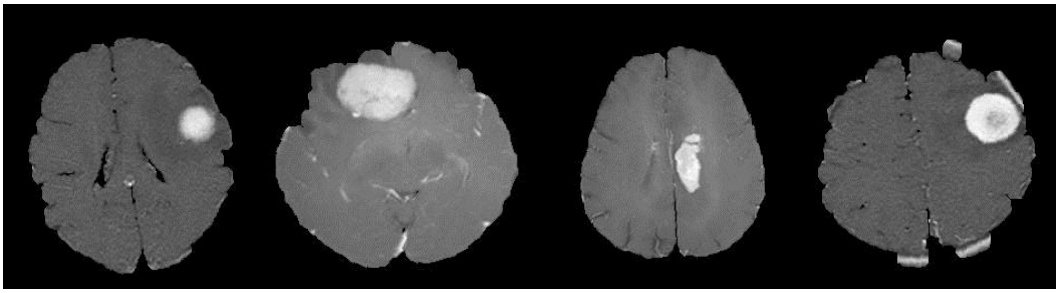

Fig. 6 Registration images

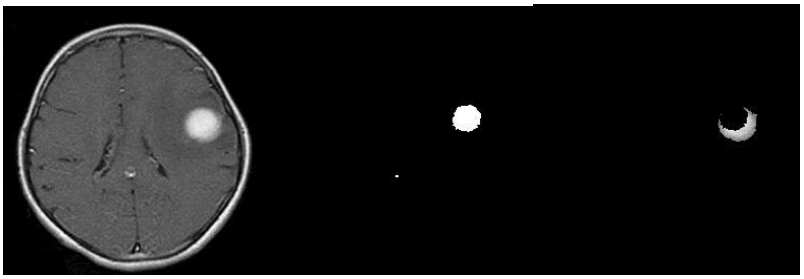

7 (a) 7 (b) 7 (c)

Fig. 7(a) Normal image, (b) Segmented tumor image, (c) Segmented edema image

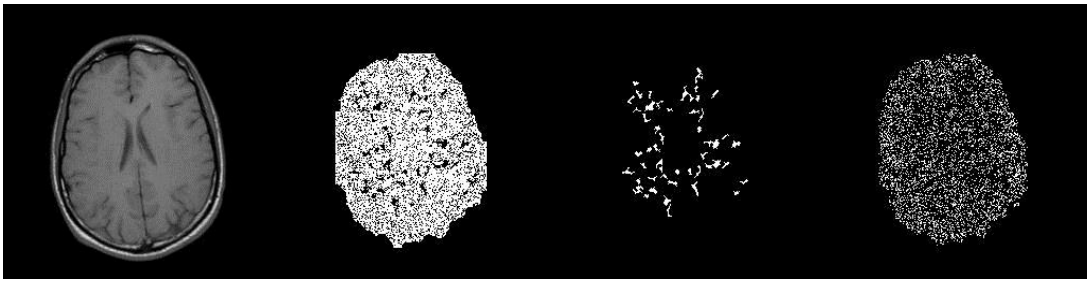

8 (a) 8 (b) 8 (c) 8 (d)

Fig. 8 (a) Abnormal image, (b) Segmented GM, (c) Segmented WM, (d) Segmented CSF

4.1 Performance analysis:

The statistical metrics of specificity, sensitivity, and accuracy is expressed as concerning the following values such as TP, FP, FN plus TN values. The execution of our suggested work is analyzed by engaging the statistical measures described below,

Accuracy:

Accuracy is defined as the proportion of true outcome; it may be either true positive or else true negative, in a population. It calculates the aggregate of the genuineness of a diagnostic test in a situation.

$$\text{Accuracy} = (\text{TN} + \text{TP})/(\text{TN} + \text{TP} + \text{FN} + \text{FP}) \tag{30}$$

Sensitivity:

Sensitivity can be well-defined as the fraction of true positives that are accurately recognized through a diagnostic test. It exhibits exactly how satisfactory the test is at detecting a disease.

$$\text{Sensitivity} = \text{TP}/(\text{TP} + \text{FN}) \tag{31}$$

Specificity:

Specificity can be well-defined as the fraction of true negatives recognized properly by a diagnostic test. It mentions exactly how satisfactory test is at identifying the normal (negative) condition.

$$Specificity = TN/(TN + FP) \tag{32}$$

False Discovery Rate:

FDR can be designated as the desired fraction of false negatives among the complete hypothesis rejected.

$$FDR = \frac{FP}{FP + TP} \tag{33}$$

False positive rate:

FPR can be well-defined as the ratio between the number of negative events incorrectly classified as positives and the sum of a number of real negative events FP and TN respectively.

$$False\ Positive\ Rate = \frac{FP}{FP + TN} \tag{34}$$

Positive predictive value:

A Positive Predictive Value (PPV) is defined as the possibility that objects with an accurate test result really has a specific object. PPV is generally denoted as a proportion,

$$PPV = \frac{TP}{TP + FP} \tag{35}$$

Negative predictive value:

A Negative Predictive Value (NPV) is defined as the probability which objects with a wrong result truly does not comprise of those specific objects. NPV is generally articulated as a proportion,

$$NPV = \frac{TN}{TN + FN} \tag{36}$$

Mathew's correlation coefficient:

MCC is defined as the true and false positives and negatives and also it is considered as a composed measure that can be employed even if the classes are of very variant sizes.

$$MCC = \frac{(TP \times TN) - (FP \times FN)}{\sqrt{(TP + FP)(TP + FN)(TN + FP)(TN + FN)}} \tag{37}$$

4.2Comparative analysis:

4.2.1 Tumor segmentation

The tumor is segmented from the unusual image utilizing enhanced FCM algorithm. In table 1 tumor segmentation utilizing Modified FCM is matched with the prevailing k means and FCM and demonstrates that our suggested tumor segmentation outcome is superior to the prevailing tumor segmentation.

TABLE I: Comparison table of tumor segmentation

Methods	Sensitivity	Specificity	Accuracy	FPR	PPV	NPV	FDR	MCC	F-measure
MFCM	0.9921	0.5836	0.9789	0.4163	0.9865	0.7741	0.0134	0.6119	0.9891
FCM	0.9888	0.5109	0.9736	0.4890	0.9843	0.5758	0.0156	0.4837	0.9864
Kmeans	0.9870	0.4949	0.9715	0.5050	0.9838	0.4899	0.0161	0.4418	0.9853

The comparison table 1 denotes that the accuracy, sensitivity, specificity of our suggested technique is higher than the prevailing method K-means and False Rates are also considerably diminished when matched with the prevailing K-means, and FCM methods. The comparison graph is shown as follows in fig. 9,

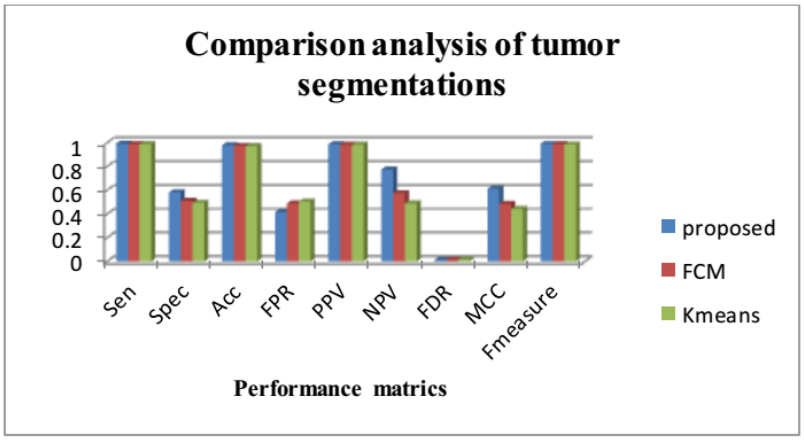

Fig.9 Comparison graph of tumor segmentations

4.2.2 Edema segmentation

Edema region is apportioned from the abnormal image utilizing modified region developing algorithm. In table 2, edema segmentation utilizing Modified region growing is coordinated with the prevailing region growing method and evidence that our proposed edema segmentation consequence is superior to the former edema segmentations.

TABLE II: Comparison table of edema segmentation

Methods	Sensitivity	Specificity	Accuracy	FPR	PPV	NPV	FDR	MCC	F-measure
MRG	0.9968	0.7096	0.9924	0.2903	0.9955	0.7901	0.0044	0.7249	0.9961
RG	0.9907	0.8396	0.9889	0.1603	0.9979	0.6924	0.0020	0.7387	0.9943

The comparison table 2 shows that the accuracy, sensitivity, specificity of our suggested modified region growing segmentation result is higher than the existing method region growing method and False Rates are also considerably diminished when matched with the present region growing technique. The comparison graph is represented in fig. 10,

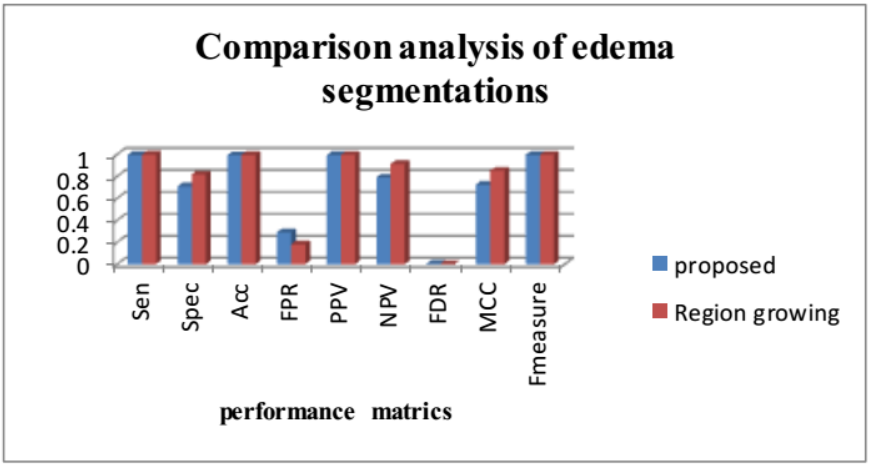

Fig. 10 Comparison graph of edema segmentations

4.2.3 GM, WM and CSF segmentations

GM, WM and also CSF are apportioned from the usual images and also the statistical measures are calculated for all segmentation. The suggested segmentation performance metric outcomes are enumerated in table 3.

TABLE III: Results of GM, WM and CSF segmentations

Segmentation	Sensitivity	Specificity	Accuracy	FPR	PPV	NPV	FDR	MCC	F-measure
GM	0.8815	0.5113	0.8330	0.4886	0.9235	0.4330	0.0764	0.3708	0.9003
WM	0.9957	0.9218	0.9836	0.0781	0.9847	0.9663	0.0152	0.9339	0.9901
CSF	0.9680	0.8906	0.9658	0.1093	0.9963	0.6504	0.0036	0.7262	0.9815

4.2.4 Classification

The performance of the projected classifier FFNN outcomes compared with the existing SVM and NB classifiers in the case of statistical measures such as accuracy, sensitivity, specificity, FPR, FDR, PPV, NPV, MCCand the table for the comparison results have been specified in the following table 4.

TABLE IV: Comparison table of classification

MEASURES	PROPOSED[FFNN]	EXISTING[SVM]	EXISTING[NB]
Sensitivity	0.777778	0.288889	0.378378
Specificity	0.981132	0.923077	0.970588
Accuracy	0.929577	0.521127	0.661972
FPR	0.018868	0.076923	0.029412
PPV	0.933333	0.866667	0.933333
NPV	0.928571	0.428571	0.589286
FDR	0.066667	0.133333	0.066667
MCC	0.808769	0.250161	0.427056
F measure	0.433333	0.538462	0.848485

The comparison table 4 presents that the accuracy, sensitivity, specificity of our projected modified region growing segmentation end result which is greater than the prevailing system of region growing methodology and henceforth the False Rates are suggestively compact when compared with the prevailing region growing technique. The below graph represents the comparison of various classifiers performances and it is shown in fig. 11,

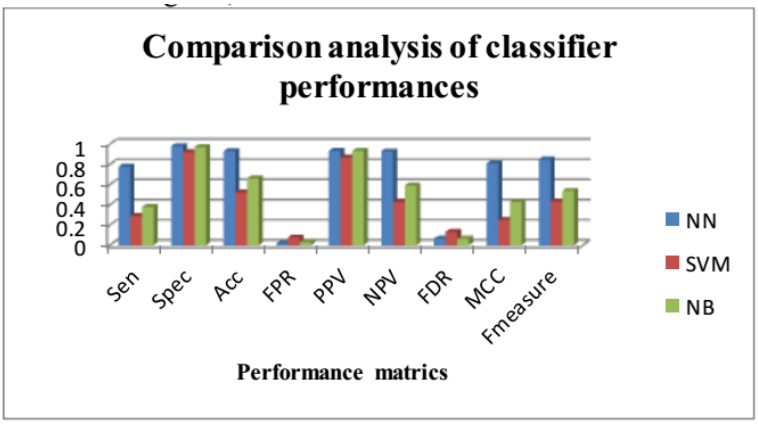

Fig. 11 Comparison graph of classifier performances

The above graph exhibits the recommended classifier and FFNN gives good classification outcome than the former SVM and as well the classifiers specifically as Naive Bayes classifiers.

CONCLUSION

On account of our proposed methodology, we have suggested efficacious classification of MRI and also segmentations utilizing amended algorithms and also this task diminishes the intricacy of prevailing techniques in both segmentation and also classification. Furthermore, in comparative evaluation, our suggested technique is matched with the prevailing techniques regarding the performances in case of accuracy, sensitivity, and specificity, FPR, PPV, NPV, FDR and also MCC. The comparison outcomes present that our suggested work segmentations applying modified algorithms and also classification utilizing FFNN classifier has effectively classified the MRI images than the prevailing techniques.

REFERENCES

[1] S.K. Bandyopadhyay, and T.U. Paul, "Automatic segmentation of brain tumour from multiple images of brain MRI", International Journal of Application or Innovation in Engineering & Management (IJAIEM), vol.2, no.1, 2013

[2] J.S. Sengar, and P. Chanderiya, "Review: A Survey on Brain Tumor Extraction from MRI", International Journal of Signal Processing, Image Processing, and Pattern Recognition, vol.9, no. 6, pp.171-176, 2016

[3] D. Bhattacharyya, and T.H. Kim, "Brain tumor detection using MRI image analysis", In International Conference on Ubiquitous Computing and Multimedia Applications, pp. 307-314, Springer Berlin Heidelberg, 2011

[4] S. Nag, I.K. Maitra, M. Sudipta, and K. Bandyopadhyay, "A review of image segmentation methods on brain MRI for detection of tumor and related abnormalities", International Journal of Advanced Research in Computer Science and Software engineering, vol.4, pp.1073-1095, 2014

[5] P.S. Swathi, D. Devassy, V. Paul, and P. N. Sankaranarayanan, "Brain Tumor Detection and Classification Using Histogram Thresholding and ANN", International Journal of Computer Science and Information Technologies, vol.6, no.1, pp.173-176, 2015

[6] R. Aggarwal, A. Kaur, "Efficient Analysis of Brain Tumor Detection and Identification Using Different Algorithms", International Journal of Engineering Sciences & Research technology, vol.3, no.5, 2014

[7] G. Madhikar, and S.S. Lokhande, "Brain Tumour Detection and Classification by Using Modified Region Growing Method: A Review", In International Journal of Engineering Research and Technology, vol.2, no.12, 2013
[8] M. Tahir, A. Iqbal, A.S. Khan, "A Review Paper of Various Filters for Noise Removal in MRI Brain Image", International Journal of Innovative Research in Computer and Communication Engineering, vol. 4, no. 12, 2016
[9] M.C. Clark, L.O. Hall, D.B. Goldgof, R. Velthuizen, F.R. Murtagh, and M.S. Silbiger, "Automatic tumor segmentation using knowledge-based techniques", IEEE transactions on medical imaging, vol.17, no.2 pp.187-201,1998
[10] M. Ramesh, P. Priya, and P.M. Arabi, "A novel approach for efficient skull stripping using morphological reconstruction and thresholding techniques", Int. J. Res. Eng. Technology, vol.3, pp. 96-101, 2014
[11] S.M. Ali, L.K. Abood, and R.S. Abdoon, "Brain Tumor Detection of Skull Stripped MR Images Utilizing Clustering and Region Growing", Iraqi Journal of Science, vol. 55, no. 3A pp. 1108-1119, 2014
[12] K. Somasundaram, and P. Kalavathi, "Skull stripping of MRI head scans based on Chan-Vese active contour model", KM&EL, Vol.3, no. 1, pp.7-14, 2011
[13] E.E.M. Azhari, M.M.M. Hatta, Z.Z. Htike, and S.L. Win, "Tumor detection in medical imaging: A survey", International journal of Advanced Information Technology, vol.4, no.1, 2014
[14] A. Anand, H. Kaur, "Survey on Segmentation of Brain Tumor: A Review of Literature", International Journal of Advanced Research in Computer and Communication Engineering, vol. 5, no.1, 2016
[15] N. Gordillo, E. Montseny, and P. Sobrevilla, "State of the art survey on MRI brain tumor segmentation", Magnetic resonance imaging vol. 31, no. 8, pp. 1426-1438, 2013
[16] J. Liu, M. Li, J. Wang, F. Wu, T. Liu, and Y. Pan, "A survey of MRI-based brain tumor segmentation methods", Tsinghua Science and Technology, vol.19, no.6, pp.578-595, 2014
[17]A.R. Mathew, P.B. Anto, "A Review on MRI Brain Image Segmentation Techniques", International Journal of Innovative Research in Electrical, Electronics, Instrumentation and Control Engineering, vol. 3, no.1, 2016
[18] D. Selvaraj, and R. Dhanasekaran, "Mri brain image segmentation techniques-A review", Indian Journal of Computer Science and Engineering (IJCSE), 2011
[19] K. Sharma, A. Kaur, and S. Gujral, "A review on various brain tumor detection techniques in brain MRI images", IOSR Journal of Engineering, vol.4, no. 5, pp.6-12, 2014
[20] D .Selvaraj, and R. Dhanasekaran, "A review on current MRI brain tissue segmentation feature extraction and classification techniques." International Journal of Electronics, vol.3, pp.21-30, 2013
[21] V.anitha, S. murugavalli, "Brain tumour classification using two-tier classifier with adaptive segmentation technique", IET Computer Vision, vol.10, no.1, pp.9-17, 2016.
[22] Q. Ain, M.A. Jaffar, and T.S. Choi, "Fuzzy anisotropic diffusion based segmentation and texture based ensemble classification of brain tumor", Applied Soft Computing, vol.21, pp.330-340, 2014
[23] M. Saritha, K.P. Joseph, and T.A. Mathew, "Classification of MRI brain images using combined wavelet entropy based spider web plots and probabilistic neural network", Pattern Recognition Letters, vol.34, no.16, pp.2151-2156, 2013
[24] N. Nabizadeh, N. John, and C. Wright, "Histogram-based gravitational optimization algorithm on single MR modality for automatic brain lesion detection and segmentation", Expert Systems with Applications, vol.41, no.17, pp.7820-7836, 2014
[25] A. Chaddad, and C. Tanougast, "Quantitative evaluation of robust skull stripping and tumor detection applied to axial MR images", Brain Informatics, vol.3, no.1, pp.53-61, 2016
[26] T. Chakravorty, G. A. Bilodeau, and E. Granger, "Automatic image registration in infrared-visible videos using polygon vertices", pp. 1403.4232, 2014

